

TABLE II. Typical shock-producing systems.

Explosive ^a thickness (cm)	Attenuator thickness (cm)	Specimen-plate thickness (cm)	Pressure ^b (kbar)	Particle velocity ^b (mm/ μ sec)
3.75 CH ₃ NO ₂	...	3.75 brass	200	0.530
3.75 CH ₃ NO ₂	...	2.54 brass	227	0.580
3.75 CH ₃ NO ₂	...	1.27 brass	240	0.613
3.75 CH ₃ NO ₂	0.838 brass/0.838 Plexiglas	0.838 brass	128	0.361
3.75 CH ₃ NO ₂	1.27 brass	2.41 Plexiglas	43.0	0.900
3.75 CH ₃ NO ₂	2.54 brass	2.41 Plexiglas	36.8	0.800
1.27 Comp B	...	2.54 brass	225	0.600
1.27 Comp B	...	1.27 brass	278	0.710
1.27 Comp B	0.838 brass/0.838 hexane	0.828 brass	66.1	0.201

^a Diam 13.9 cm.^b Shock-wave parameters of specimen plate.

aluminized side of the film was held to the specimen surface by an extremely thin layer of silicone grease.

A dual-slit system was used in the camera. The images of the two slits (Fig. 2) were parallel to each other and equally spaced on each side of the center of the specimen plate. Usually one slit was aligned across the test specimens, the other being used to record the free-surface motion of the specimen plate. A glass "flasher" plate, mounted a small (but accurately known) distance from the specimen-plate surface, was used to obtain the free-surface velocity.

The various shock-producing systems (Table II) were calibrated by using free-surface-velocity measurements of specimen plates and the corresponding shock-wave velocities obtained from the known equations-of-state of specimen-plate materials.¹⁴ The calibrations were checked and refined by frequently including samples of the specimen-plate material in the same experiments with the explosive specimens. The shock transit times within the specimens were determined from the intensity changes occurring in the reflected light when the shock wave arrived at the free surface.¹⁵ These times were divided into the specimen heights to obtain mean shock-wave velocities. By this method we obtained the U_s -vs- u_p relations for naval brass and Plexiglas, as well as for the explosive specimens. Naval brass is nominally composed of 59.00% Cu; 0.50%–1.00% Sn; 0.4% maximum impurity; and the remainder, Zn. For the brass (density = 8.37 g/cm³),

$$U_s(\text{mm}/\mu\text{sec}) = 3.560 + 1.833u_p, \quad (3)$$

and for Plexiglas,

$$U_s(\text{mm}/\mu\text{sec}) = 2.710 + 1.568u_p - 0.037u_p^2. \quad (4)$$

Measurements of the transit times of weak shock waves (~ 100 bar) were used to obtain "sound" wave

¹⁴ The free-surface velocity for a plane shock wave is almost twice the particle velocity. See R. W. Goranson, D. Bancroft, B. L. Burton, T. Blechar, E. E. Houston, E. F. Gittings, and S. A. Landeen, *J. Appl. Phys.* **26**, 1472 (1955); J. M. Walsh and R. H. Christian, *Phys. Rev.* **97**, 1544 (1955).

¹⁵ See N. L. Coleburn, *J. Chem. Phys.* **40**, 71 (1964) for the description and analysis of a typical record obtained using the reflected-light technique.

velocities¹⁶ in larger specimens, 1.27 cm thick by 5.08-cm diameter. In the experiment (Fig. 3) a cylinder (or slab) of the explosive is immersed in a Plexiglas aquarium. A detonator is centered 30 cm from the plane surface of the specimen. The initiation of the detonator produces a shock wave in water which is nearly plane when it arrives at the surface of the specimen. The motion of the shock wave is recorded by a smear camera using a shadowgraph technique; i.e., backlighting with collimated light from an exploding wire. The resulting record (Fig. 4) permits measuring the transit time of the shock wave in the specimen and the shock-wave velocity in the water before and after the wave enters the specimen.

IV. RESULTS

Figures 5, 6, 7, and 8 are plots of the experimental measurements of shock-wave and particle velocities in

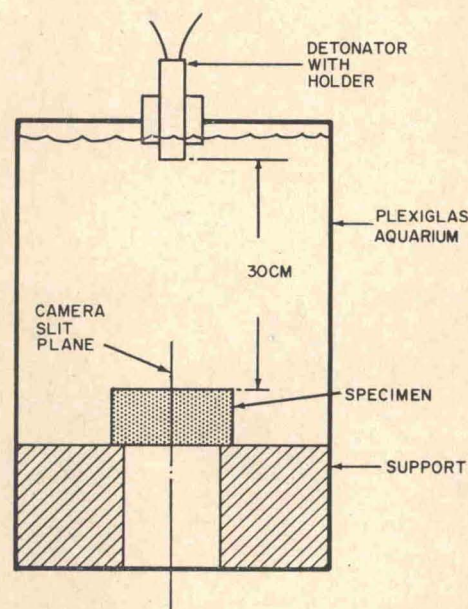


FIG. 3. Arrangement for initiating and measuring weak shock waves (~ 100 bar).

¹⁶ J. M. Majowicz, Naval Ordnance Laboratory Technical Report, NavOrd Report 4524 (1957), classified.

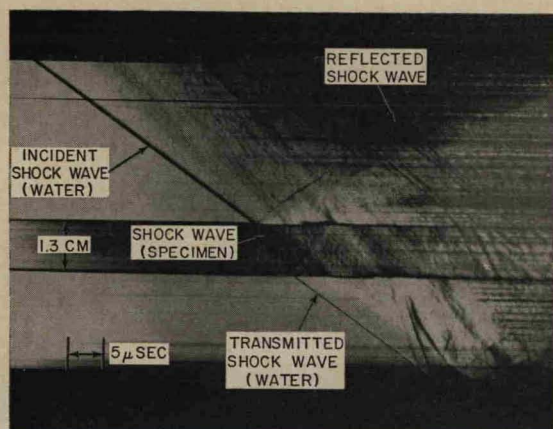


FIG. 4. Smear-camera shadowgraph of shock waves obtained using the arrangement of Fig. 3. The upper and lower traces are from the incident and transmitted shock waves in water. The central dark band denotes the specimen height. The shock trace in the specimen (Plexiglas) is seen within this band.

the CHON explosives. The measurements for the aluminized explosives and propellants are plotted in Fig. 9. The data show that the shock-wave velocity is a linear function of the particle velocity within experimental error over a wide range, i.e.,

$$U_s = A + Bu_p \quad (5)$$

from particle velocities of about 0.3 to 1.2 mm/μsec.

If Eq. (5) applies to the lower amplitude limit, $u_p = 0$, and the behavior of the material is fluidlike,

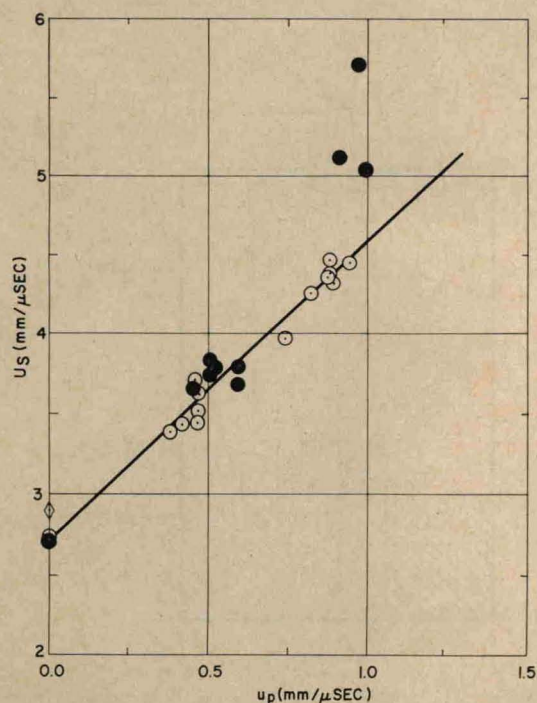


FIG. 5. Shock-wave velocity, U_s , vs particle velocity, u_p , of Composition B-3 (○), LX-04-0 (●). [PBX 9404-03 (◇), sound velocity included for comparison.]

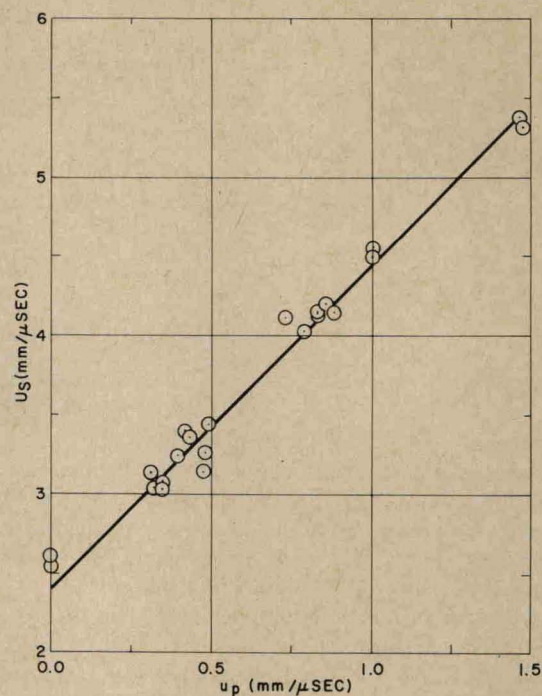


FIG. 6. Shock-wave velocity, U_s , vs particle velocity, u_p , on TNT.

then according to theory the intercept A should equal the adiabatic bulk-sound speed. Our first thoughts were that the weak-shock-velocity experiments should give good approximate values of the bulk velocities. By

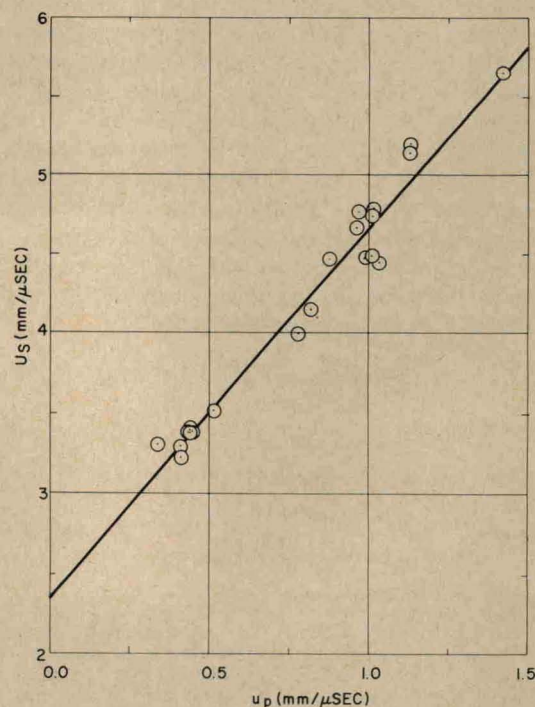


FIG. 7. Shock-wave velocity, U_s , vs particle velocity, u_p , of TATB.